CALCULATION OF OH COIL STRESSES IN THE NSTX CSU

NSTXU-CALC-133-08-01

October 17, 2013

Prepared By:

_____

Ali Zolfaghari, PPPL Mechanical Engineering
Reviewed By:

_____

Michael Mardenfeld, Design(Rev0), Peter Titus (Rev1) Engineering Analysis Division
Reviewed By:

_____

James Chrzanowski, Cognizant Engineer

PPPL Calculation Form

Calculation #   <u>NSTXU-CALC-133-08</u>   Revision #   <u>01</u> ___WP #, if any   _____

                                                         (ENG-032)

Purpose of Calculation: (Define why the calculation is being performed.)

To estimate the anticipated stresses in the upgraded NSTX OH coil in various discharge scenarios and to qualify OH design to withstand the forces.

References (List any source of design information including computer program titles and revision levels.)

[1] NSTX Structural Design Criteria Document, I. Zatz
 [2] NSTX Design Point March 2011
http://www.pppl.gov/~neumeyer/NSTX_CSU/Design_Point.html
[3] NSTX Upgrade OH Conductor Fatigue Analysis, P. Titus, Calc #NSTXU-Calc-133-09

Assumptions (Identify all assumptions made as part of this calculation.)

For the TF/OH interaction analysis, the friction ratio between the TF and OH at the interface was assumed to be 0.15. This analysis assumes no in-line joints in the copper conductor. In other words, each coil turn is wound using a single piece.

Calculation (Calculation is either documented here or attached)

Attached.

Conclusion (Specify whether or not the purpose of the calculation was accomplished.)

     Please see executive summary in the attached report.

Cognizant Engineer's printed name, signature, and date

_____

I have reviewed this calculation and, to my professional satisfaction, it is properly performed and correct.

Checker's printed name, signature, and date

_____

1.   Assure that inputs were correctly selected and incorporated into the design.

2.   Calculation considers, as appropriate:

- Performance Requirements (capacity, rating, system output)
- Design Conditions (pressure, temperature, voltage, etc.)
- Load Conditions (seismic, wind, thermal, dynamic)
- Environmental Conditions (radiation zone, hazardous material, etc.)
- Material Requirements
- Structural Requirements (foundations, pipe supports, etc.)
- Hydraulic Requirements (NPSH, pressure drops, etc.)
- Chemistry Requirements
- Electrical Requirements (power source, volts, raceway, insulation)
- Equipment Reliability (FMEA)
- Failure Effects on Surrounding Equipment

3.   Assumptions necessary to perform the design activity are adequately described
and   reasonable.

4.   An appropriate calculation method was used.

5.   The results are reasonable compared to the inputs.

**NOTE: BY SIGNING CALCULATION, CHECKER ACKNOWLEDGES THAT
THE CALCULATION HAS BEEN APPROPRIATELY CHECKED AND THAT
THE APPLICABLE ITEMS LISTED ABOVE HAVE BEEN INCLUDED AS
PART OF THE CHECK.**

<u>RECORD OF CHANGES</u>

Date	Description	Effected Sections
10/19/2011	First issue	All
10/17/2013	Rev 01- Corrected figures 5B and 5C for the correct currents 13kA in OH and 16.6kA in PF1A	Figures 5B and 5C

Executive Summary

The objective of this analysis was to estimate the anticipated stresses in the upgraded NSTX OH coil in various scenarios. Axisymmetric one-way coupled structural /Emag modeling of the OH coil and interaction with PF coils were performed using ANSYS. The OH coil was modeled both as a volume with smeared property and as discrete conductors and insulation volumes. Additionally the maximum stress in the OH coil due to thermal expansion in the TF coils was calculated. This stress results from the fault scenario where the OH coil which is wound on the TF bundle, fails to energize, while the TF bundle is energized and expands outwards and upwards thermally. The frictional interaction between the TF and OH coil "drags" the OH coil with the expanding TF and causes unacceptably large tensile stresses in the OH. This was found to be true even with a low friction material interface. Consequently a gap between the two coils has been introduced. This is accomplished through the use of a water soluble layer applied on the TF on which the OH is wound. Water jets are then used to remove the layer.

Analysis with normal operating load shows that the OH coil can withstand hoop stress and shear stress at I=24kA. The analysis also revealed that in order to run the PF1A coil at 16.6 kA concurrently with the OH coil, the current in the OH will need to be limited to 13kA.

In analyzing the cooling stresses, we also pointed out the need to equalize flow velocity in the inner and outer OH turns in order to avoid large thermal stresses in the OH coil winding. In the bottom of the coil where cold water enters the coil that has been heated to near 100 Deg C due to the current and where the coil is attached to a cold G-10 base, stress in small localized regions in the insulation exceeds the limit. This also happens in the turn to turn electrical braze joints shown in the last section of the report. It is recommended that we manage the cooling scenario by preheating the cooling water in order to bring the stresses below the limit.

Introduction

The main structural loads on the OH coil and the center stack components are the results of electromagnetic (EM) forces and differential thermal expansion. The EM forces in the OH coil result from the hoop forces and the axial compression in the coil. In addition, the field from nearby coils especially the PF coils exerts force on the OH coil windings. Since the OH in NSTX upgrade is directly wound on the TF inner leg bundle, the thermal expansion in the TF in fault cases where the OH is not energized (and remains cold) causes stress in the OH. In the calculations reported here, the OH design analyzed is the latest and final design of the OH reported in
http://www.pppl.gov/~neumeyer/NSTX_CSU/Design_Point.html and whose detail are in the Design Point Spreadsheet:

Calculation

OH Stress Analysis

To study EM and thermal expansion loads on the OH coil, an axisymmetric discrete-conductor finite element model of the entire OH coil was developed. Figure 1 is a section of this model showing the finite element mesh of the copper (dark blue), epoxy insulation (light blue), and air (green). Air was meshed for electromagnetic simulation. Ansys Multiphysics FEA code was used to study the EM, structural and thermal effects.
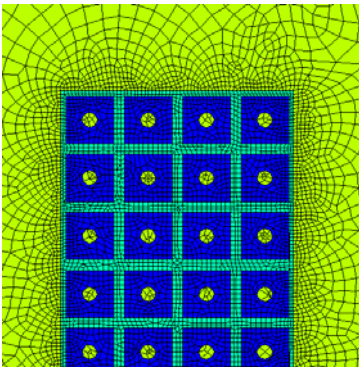

Figure 1: Finite Element Mesh Used in Axisymmetric Structural Analysis of the OH coil
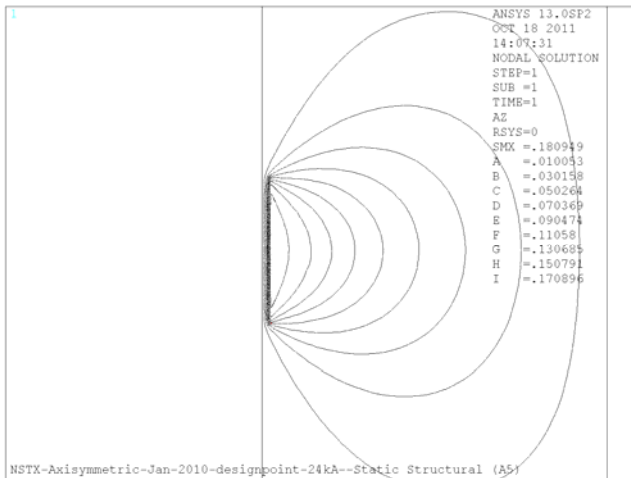
Figure 1A: Magnetic field lines

Figure 1A is a plot of magnetic flux lines of the OH solenoid magnetic field. Figure 1B and 1C are plots of the B-field at the top of the OH coil. . Table 1 lists the material properties used in the analyses used in this calculation.

Figure 2 is a plot of hoop stress in the coil at 24kA resulting from Emag (Lorentz) loads. The stress is below 125 MPa fatigue allowable stress limit for OH copper conductor. Figure 3 is a plot of the mid-plane (Tresca) stress intensity resulting from the combination of hoop and axial stresses. The stress is below the static allowable in the copper and therefore acceptable. A discussion of the fatigue analysis will follow. Figure 4 is a contour plot of shear stress in the coil epoxy insulation which is shown to be below the 10 MPa shear-stress allowable limit for CTD 425 system with primer.
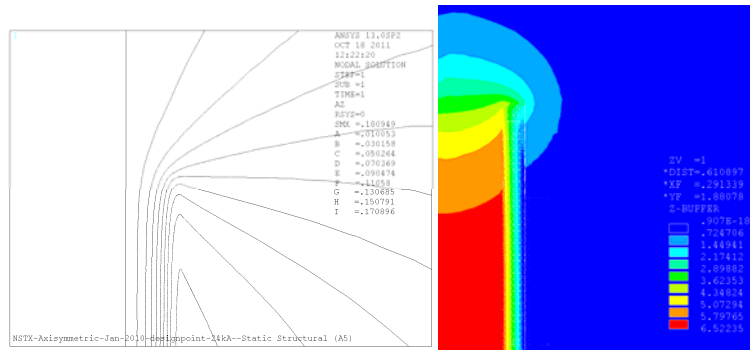
Figure 1B and 1C: Magnetic flux lines and field contours of OH solenoid at 24kA
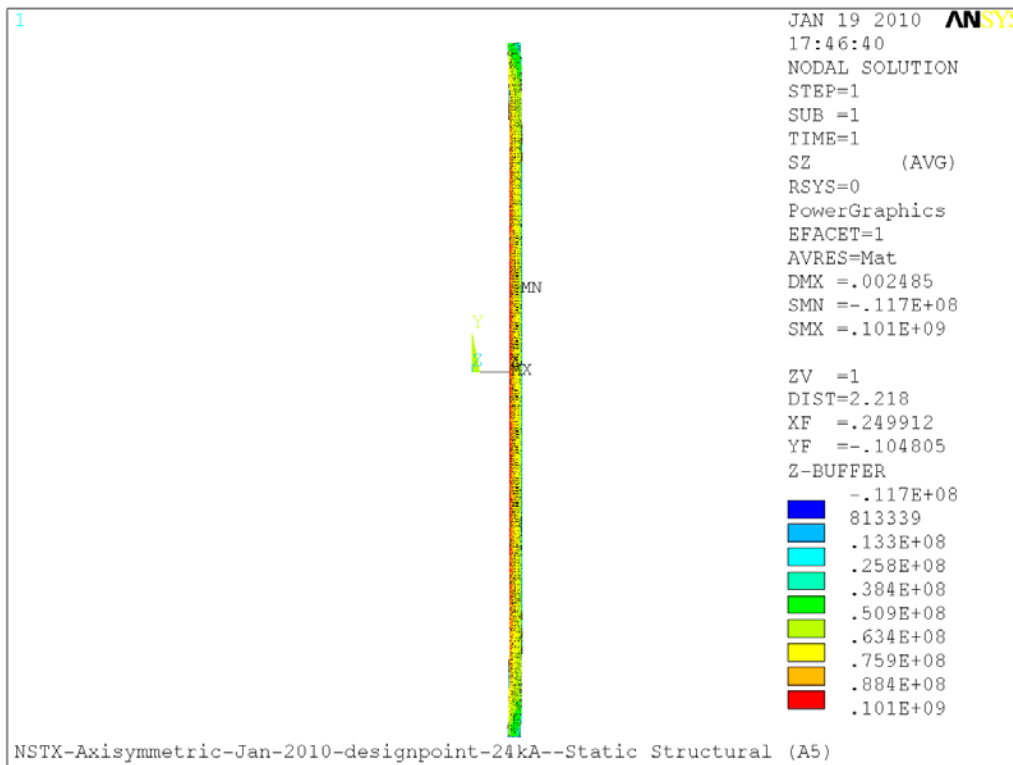
Figure 2, Hoop Stress under Emag loads

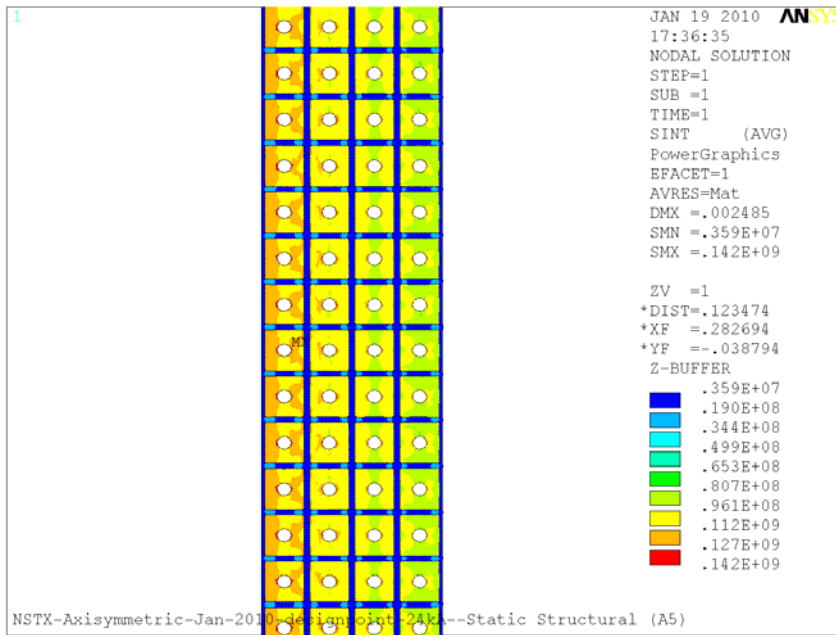| Material	Copper	Epoxy	G-10
Elastic Modulus	1.10E+11	2.20E+10	2.20E+10
Poisson's Ratio	0.32	0.145	0.145
Coef. Of therm. Expans	1.70E-05	1.40E-05	1.40E-05
Thermal Conductivity	400	0.5	0.5
Mag. Permeability	1.00E+00	1.00E+00	1.00E+00

Table 1: Material properties, All units are in MKS
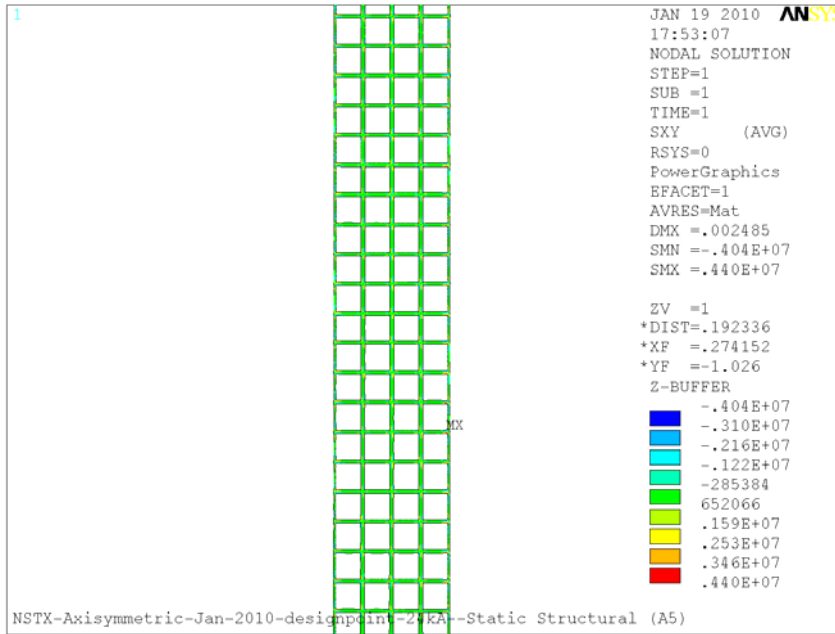

Figure 3: Stress intensity under Emag load

Figure 4: Insulation shear stress under Emag load

Conductor Fatigue Analysis

Ref[3] includes a detailed analysis of the fatigue in the OH conductor. NSTX structural criteria, and the GRD require fatigue to be addressed. The criteria allows either SN or fracture mechanics evaluations of fatigue. For SN evaluations, the more restrictive of 2 on stress and 20 on life must be met. For the Fracture mechanics evaluation a factor of 2 on flaw size, 1.5 on fracture toughness, and 2 on life must be met. The stress levels in the NSTX-U OH coil satisfy the fracture mechanics criteria, and therefore satisfy the NSTX structural requirements. Table 2 below from Ref[3] summarizes this information.

Criteria	Stress Level ant Type	Actual	
SN 2 on stress	112 MPa (Tresca)	142	Fails
SN 20 on life	180 (Tresca)	142	Passes
Fracture Mechanics with a flaw size less than .7mm 1.5 on KIc and 2 on Cycles	140 MPa (Max Principal or Hoop)	101	Passes
4 on cycles	125 MPa (Max Principal or Hoop)	101	Passes

Table 2

Effect of PF1A

Figure 5 is the plot of magnetic flux lines resulting from the OH interaction with the poloidal field coils PF1A (Upper and Lower) which is housed close to the OH coil inside the center stack housing. The plot is for a case where the OH coil current is 13 kA and PF1A coils carry 16.6 kA current. Figure 5A is the plot of the B-field magnitude in the upper portion of the OH coil.
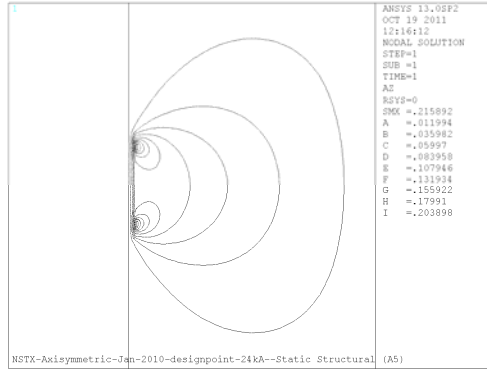
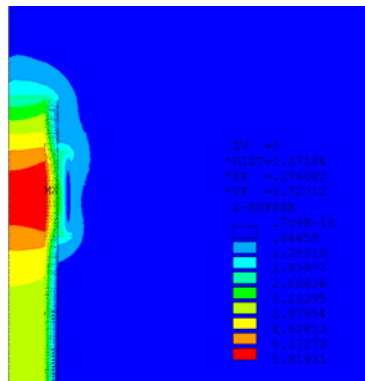Figure 5 Magnetic flux lines with PF1A on

Figure 5A; Magnetic field contours with PF1A on

Figure 5B shows the stress intensity in the OH winding resulting from the interaction. The plot shows the stress in the copper is below the allowable stress limit. From the results of analyses with this model we derived criteria limiting the currents that can flow in the OH and PF1A coils at any one time during the discharge in order to avoid damaging the OH coil. Figure 5C is the plot of the hoop stress in the coil in the vicinity of PF1A for the same conditions of Figure 5B.
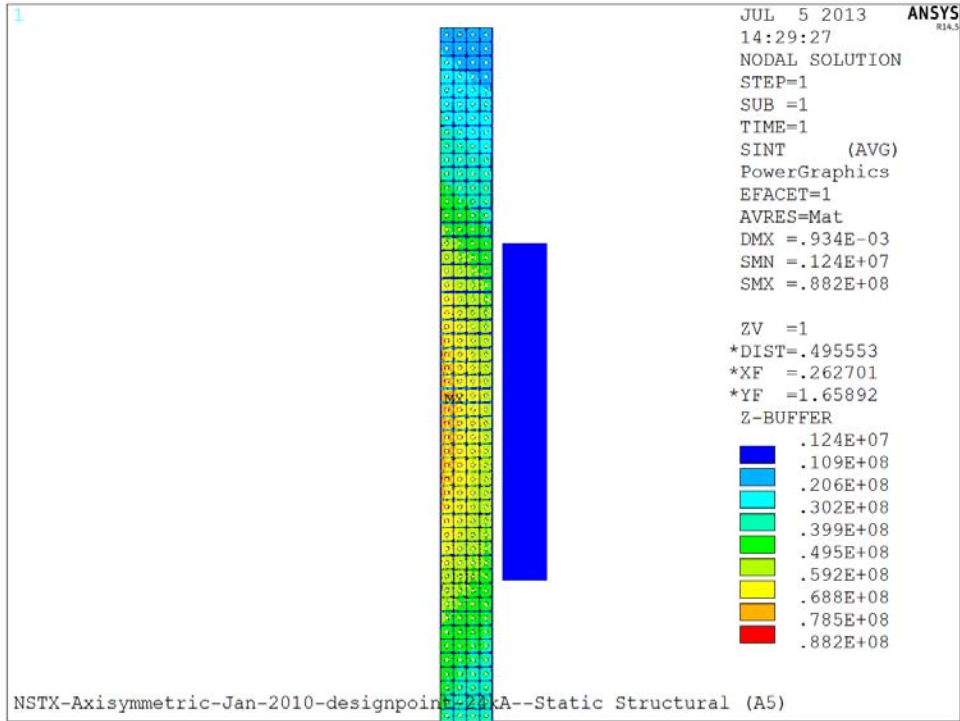
Figure 5B: Stress Intensity in the OH Coil Due to Self Currents and Interaction with Current in Adjacent PF1A Poloidal Field Coil
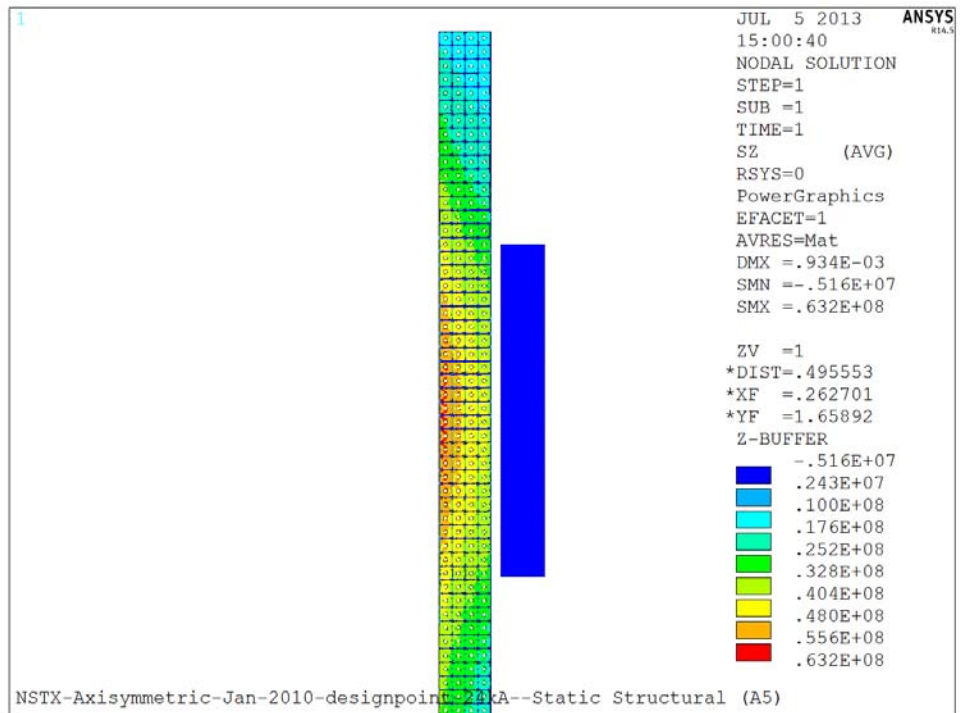
Figure 5C: Hoop stress in the OH coil due to Self Currents and Interaction with Current in Adjacent PF1A Poloidal Field Coil

Determination of Minimum Yield Strength for OH Conductor

To determine the minimum necessary yield strength in the OH conductor we calculated the average of the Tresca stress across the mid-plane of the coil. Figure 3 is a plot of stress intensity in the coil. We take a path through the mid-plane (where stress intensity is maximum) of the coil and plot the stress intensity in the copper across the path. Figure 6 is a plot of stress intensity in the copper across this path. The average value of the stress values in this plot is 107 MPa. We did the same thing for the area of the coil adjacent to the PF1A coil in order to see if the stress in that area is more limiting. Figure 7 is a plot of stress intensity along a path across the coil cross section at a height where the stress from Figure 5B is maximum. The average value of stress intensity in this plot is 99 MPa. Therefore, the mid-plane average stress of 107 MPa is more limiting. Allowing 10% for 100 deg. C operation and 10% for DCPS this S_m is 128.4 MPa. With S_m being $2/3*S_y$, the minimum S_y needs to be 193 MPa or 28 ksi.
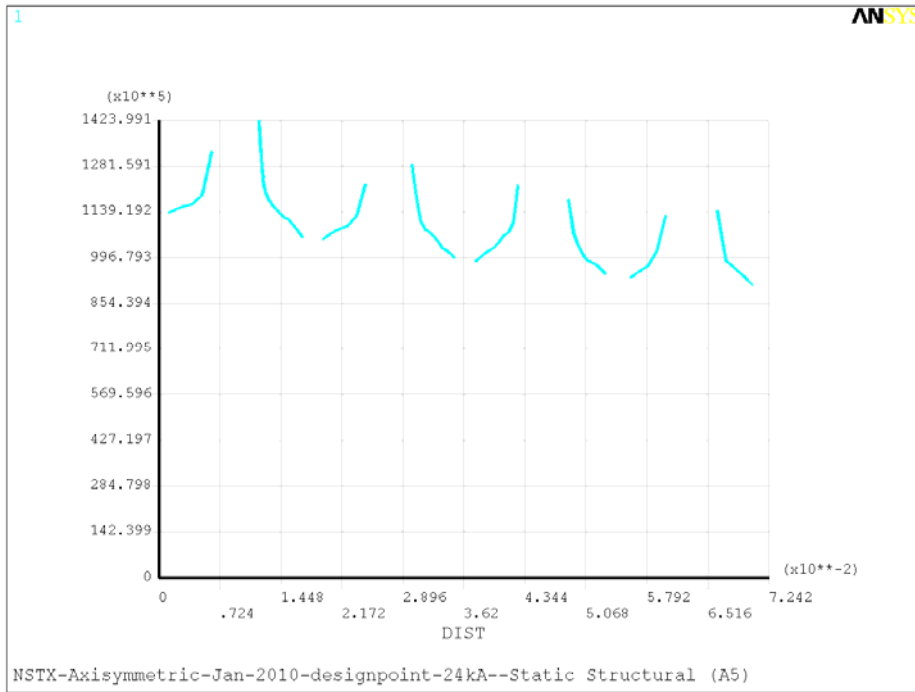
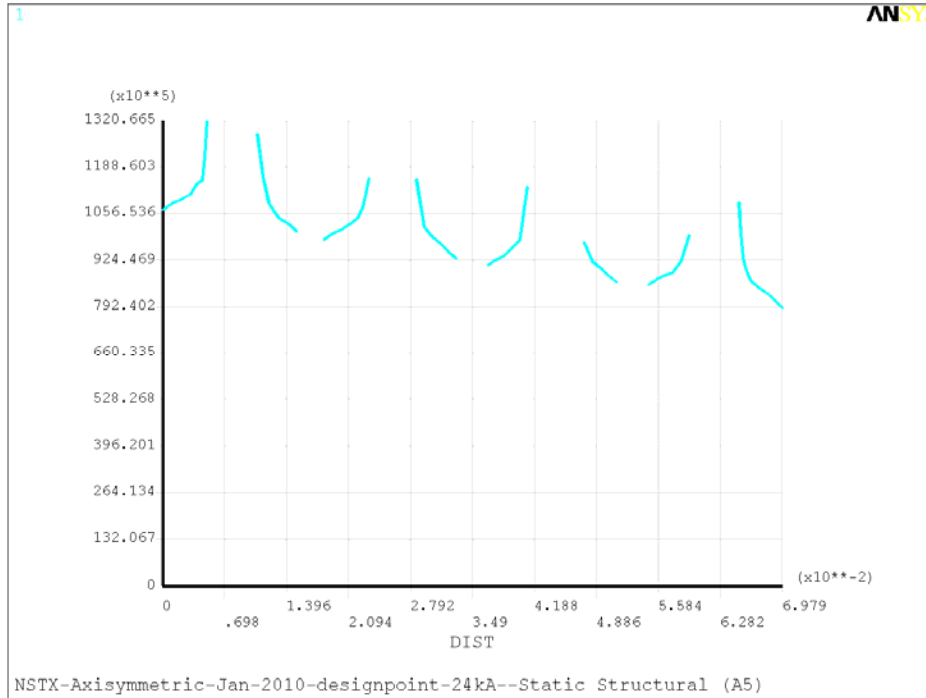Figure 6: Plot of copper stress intensity vs. radius in the mid-plane of the coil

Figure 7: Plot of copper stress intensity vs. radius in the coil adjacent the PF1A coil

Analysis of TF/OH Interaction

The OH coil in NSTX upgrade is directly wound on the TF inner legs bundle and preloaded against the TF flag extensions using Bellville spring washers.
The spring washer stacks need to be designed such as to keep the OH coil from lifting (and breaking the leads in the bottom) under all possible machine operation scenarios. Calculation number NSTX-CALC-133-04-00 by Peter Rogoff covers the design of the spring washer stacks.

In fault cases where the OH is not energized and the TF is energized (hot) the thermal expansion in the TF causes stress in the OH which is wound directly on the TF inner legs. To study this we developed two models. First model was an axisymmetric model of the center stack components in which OH was modeled as smeared property cylinder (rectangle in axisymmetry). The Bellville washer stacks were modeled as axisymmetric spring elements in the FEA model. Figure 8 shows the center stack components and this axisymmetric FEA model.
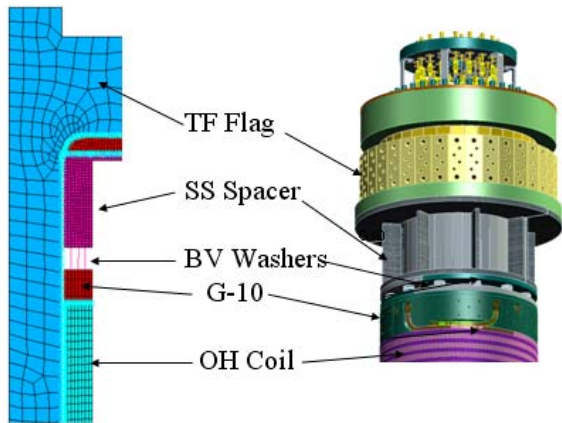
Figure 8

The second model developed was an axisymmetric coupled EM-structural Ansys FEA model in which the OH was modeled as discrete copper and insulation elements. (figure 9).
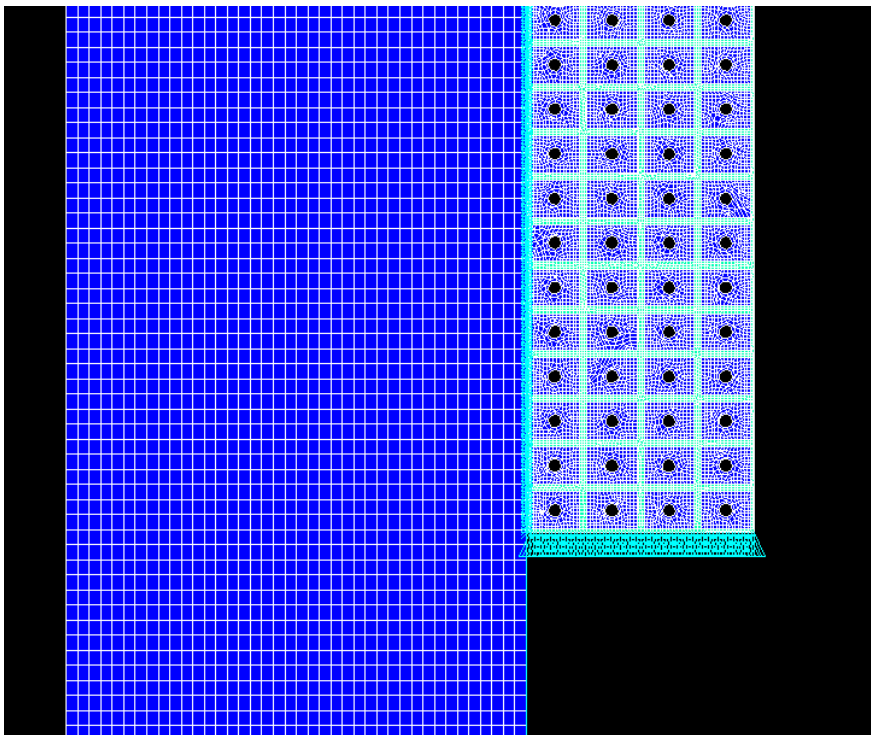

Figure 9

The TF inner leg bundle was modeled as a thick copper tube with contact elements between the TF and OH mesh with a friction ratio of 0.15. OH was held fixed in the bottom and preloaded on the top with 100,000 lbs. The model was simulated with cold

OH, and TF temperature allowed to rise from 12 to 100 deg. C. Figure 10 shows the resulting stress in the coil and the shear stress in the insulation on top portion of the coil. These stress values are acceptable.
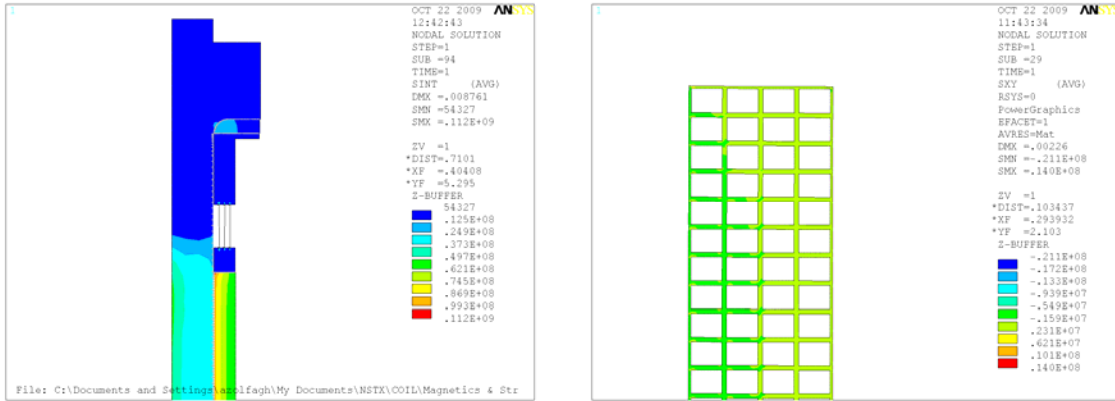
Figure 10

However, as Figure 11 shows the frictional shear of the expanding TF coil causes large unacceptable vertical tension stress in the OH. Mechanical solutions such as low friction interface and removable interface layer as well as solutions in the coil protection system need to be considered to avoid this problem.
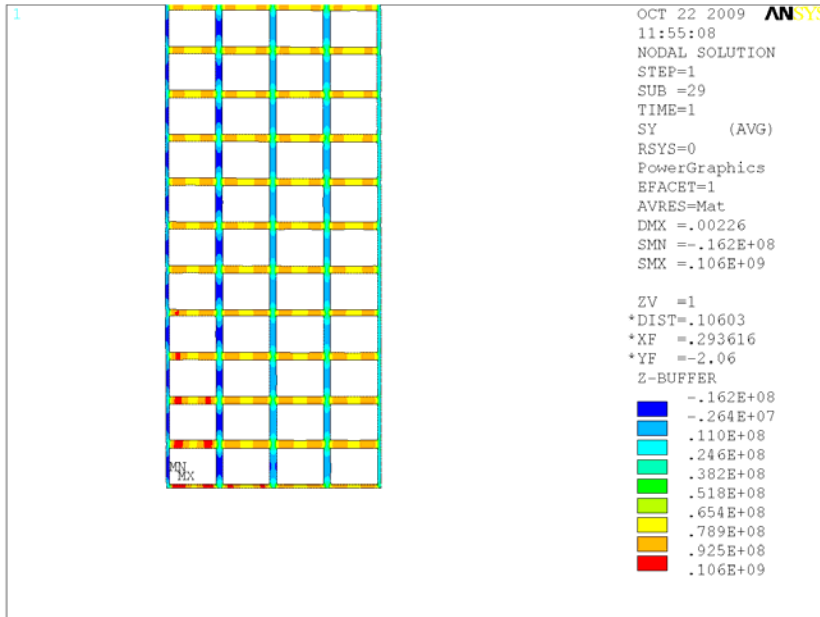
Figure 11

Stresses Induced by Differential Cooling between Inner and Outer turns:

 Another phenomena which exerts stresses in the OH coil is the differential cooling stresses also discussed in NSTXU-CALC-133-06-00 which are caused by the inner turns of the coil which have shorter lengths cooling down faster than the outer turns that are longer.
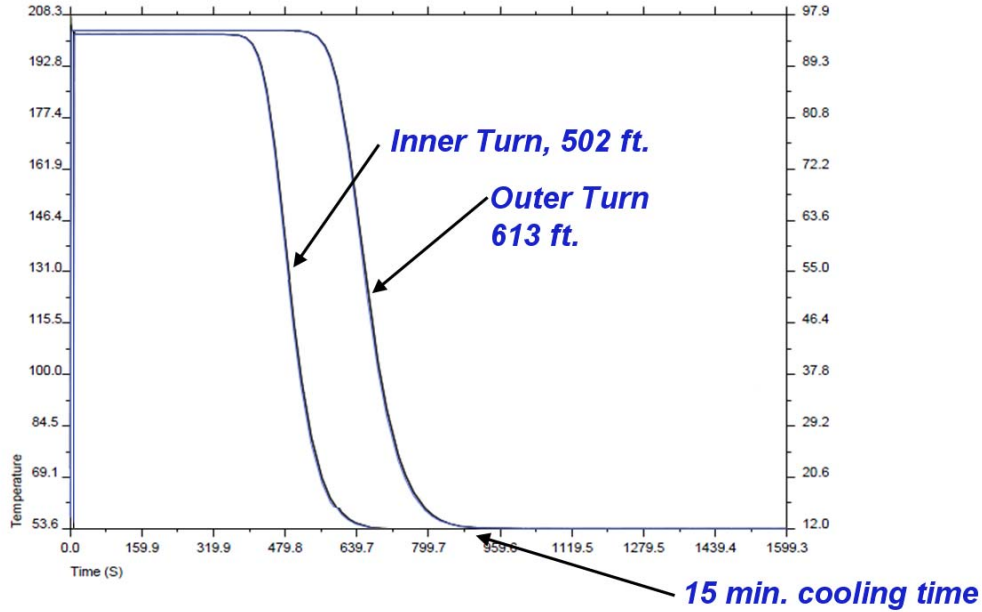
Fig. 12: Superposition of cooling plot for the shortest and longest cooling paths.

Fig. 12 is a superposition of the cooling curves for the longest path (outside layer) and the shortest cooling path (inside layer) for 430 psi pump pressure. The figure shows that at 700 seconds into the cooling, at the end of the coil (i.e. top of the coil), the inner layer has cooled down completely while the outer layer is still at the peak temperature. This was identified as a possible source of thermal stress on the coil structure. To study this effect we used an Ansys axisymmetric FEA model of the end of the coil with imposed temperatures of 12, 40, 70, and 100 deg. C on the layers. Figure 13 shows the model and the corresponding mesh.
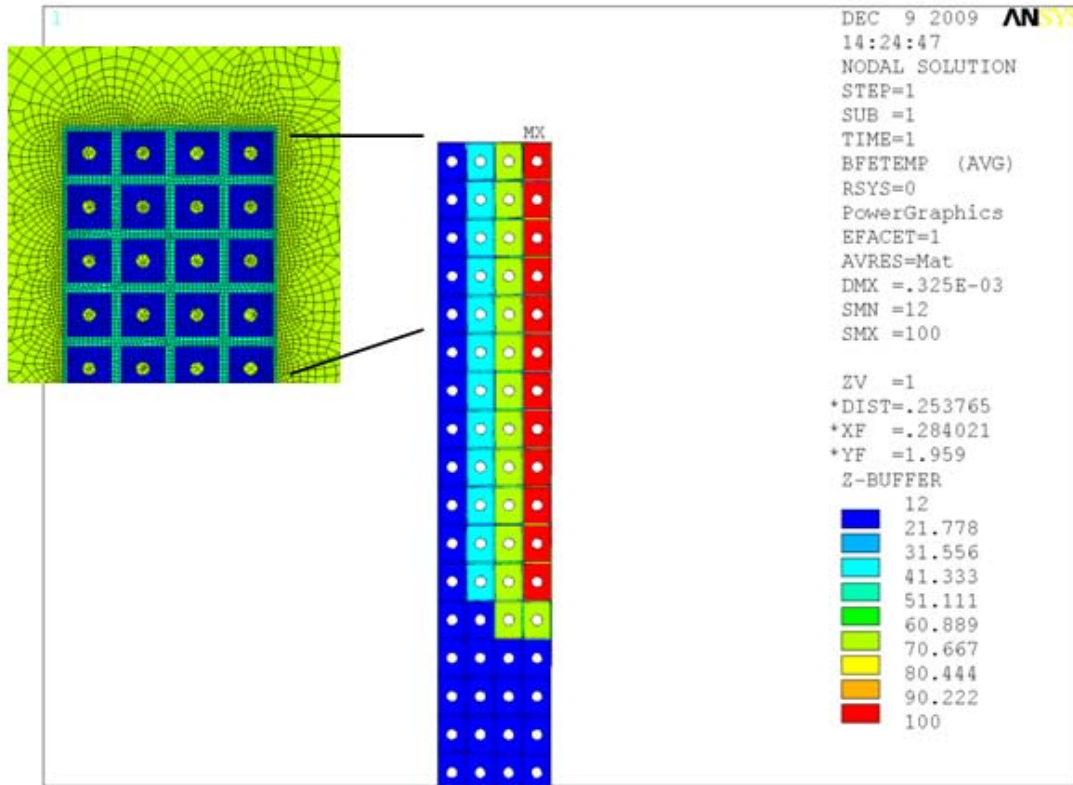
Fig. 13: Ansys FEA axisymmetric model of the end of the OH coil

Figure 14 shows the resulting stress intensity in the OH copper conductors. The stresses are high but below the 193 MPa static limit for copper. However fatigue becomes an issue with this level of stress. Figure 15 shows the resulting stress in the epoxy insulation between the conductors. The figure shows areas on the inside of the OH coil where the tension stresses are beyond the limits for epoxy. For these reasons we must avoid this situation altogether by throttling the flow speed in the short inside layers (e.g. by using pressure reduction valves) to equalize the flow velocity and thereby cooling wave velocity in the layers.
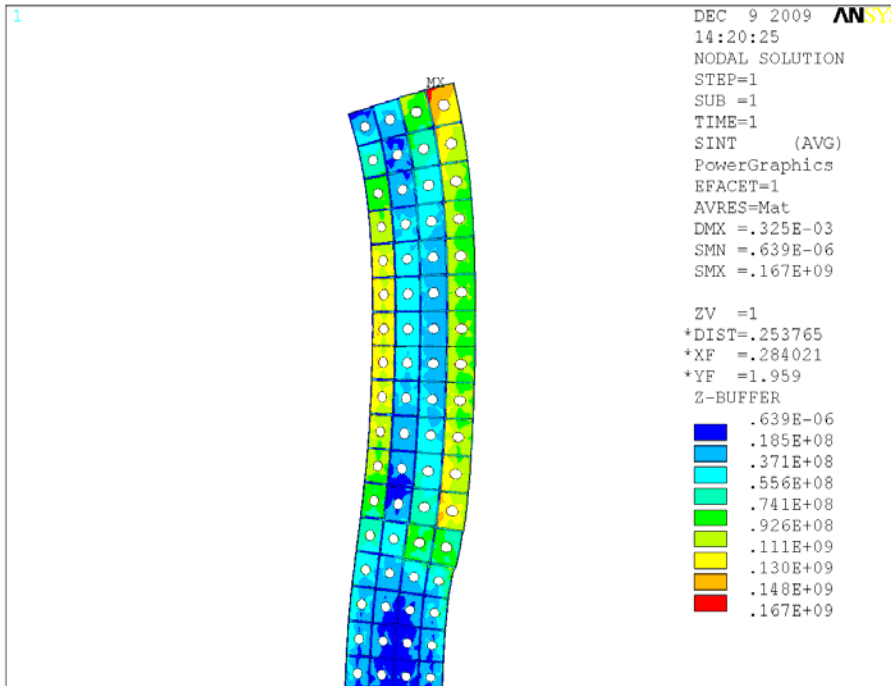
**Fig. 14: Thermal stress in the OH coil**
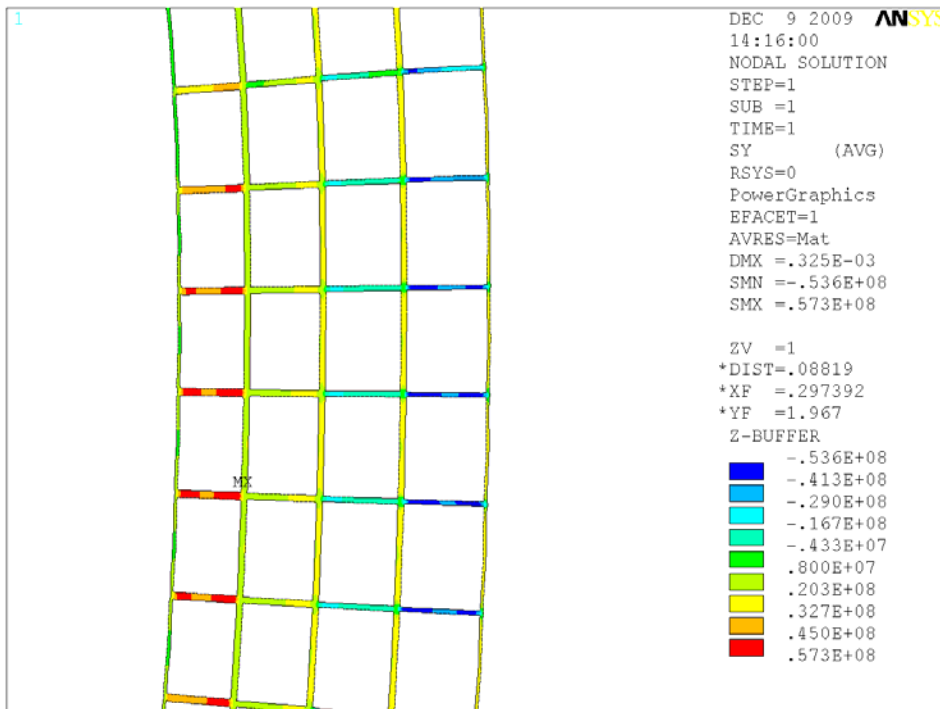
Fig. 15: Thermal stress in the OH coil insulation

Digital Coil Protection System (DCPS) Input

Input to the DCPS will be developed based on the OH stress calculations as done in the NSTX Upgrade design point spreadsheet (worksheet "Base") [2]. The advantage of this method is that OH stresses can be calculated algebraically based on current, coil dimensions. The max principal stress (i.e. hoop stress, see figure 2) in the conductor must be kept below 125 MPa and in the insulation below 10MPa.

Stresses Induced by Cold Water Entering the Hot Coil after the Shot

The temperature of the coil reaches close to 100 C in a few seconds but the water entering the coil (from the bottom of the coil) is at 12 degrees C. As the colder water moves through the coil, it creates a temperature gradient in the coil that causes stress in the coil. To study this effect we analyzed the results of cooling in the inner most layer of the OH coil. The highest temperature gradient (as calculated by Fcool) over the first 4 turn (each turn is 1.378 m) of the coil happens at t=5.96 seconds after the start of the shot and is shown in Figure 16.
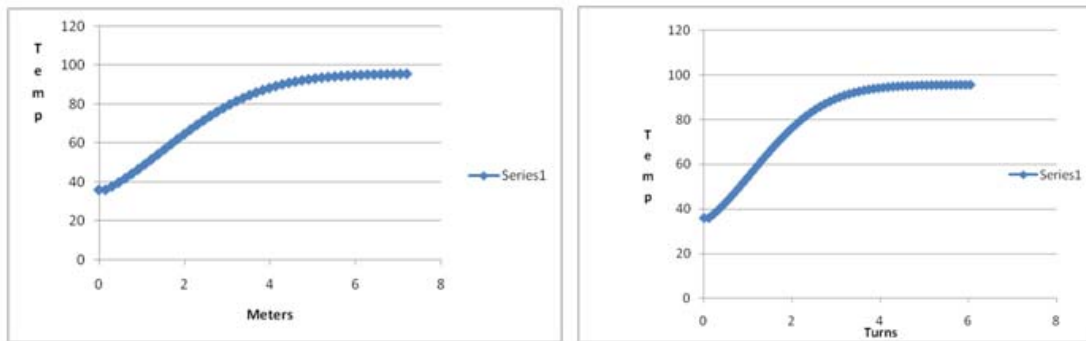
Fig. 16: Thermal gradient during transient cooldown in the bottom of the coil

The highest slope over the linear portion of the gradient is approximately 20 deg. C per turn. Figure 17 shows this temperature gradient imposed on the axisymmetric detailed FEA model of the bottom of the coil. The bottom of the coil in the model is attached to the G-10 base. The bottom of the base is kept fixed in the vertical (Y) direction and free from expansion in the radial (X) direction.
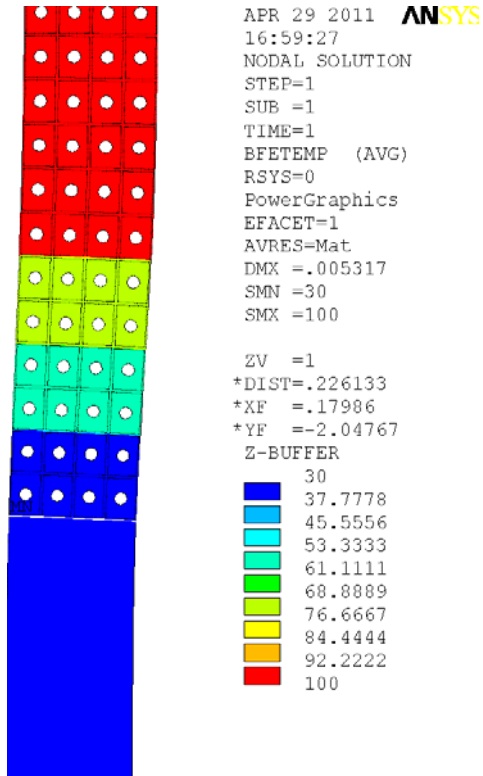
Fig. 17

Figure 18 and 19 show the contours of normal stress in the Y direction and XY shear stress.
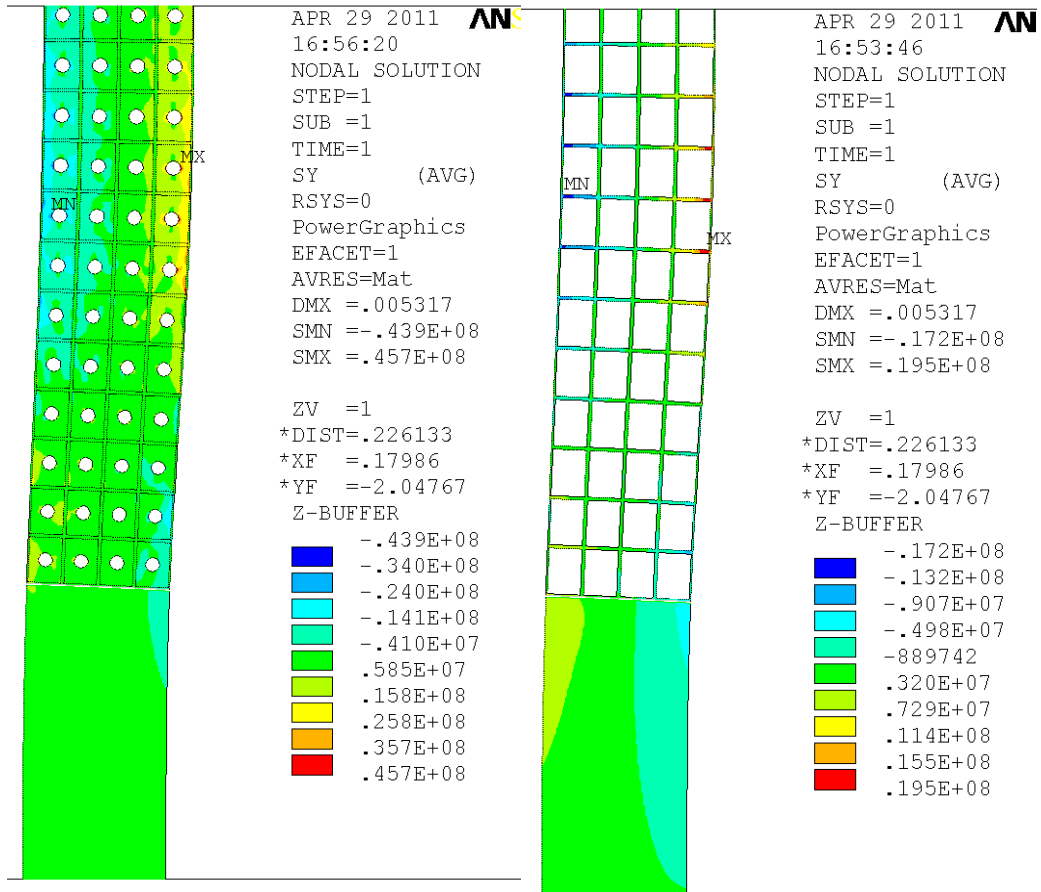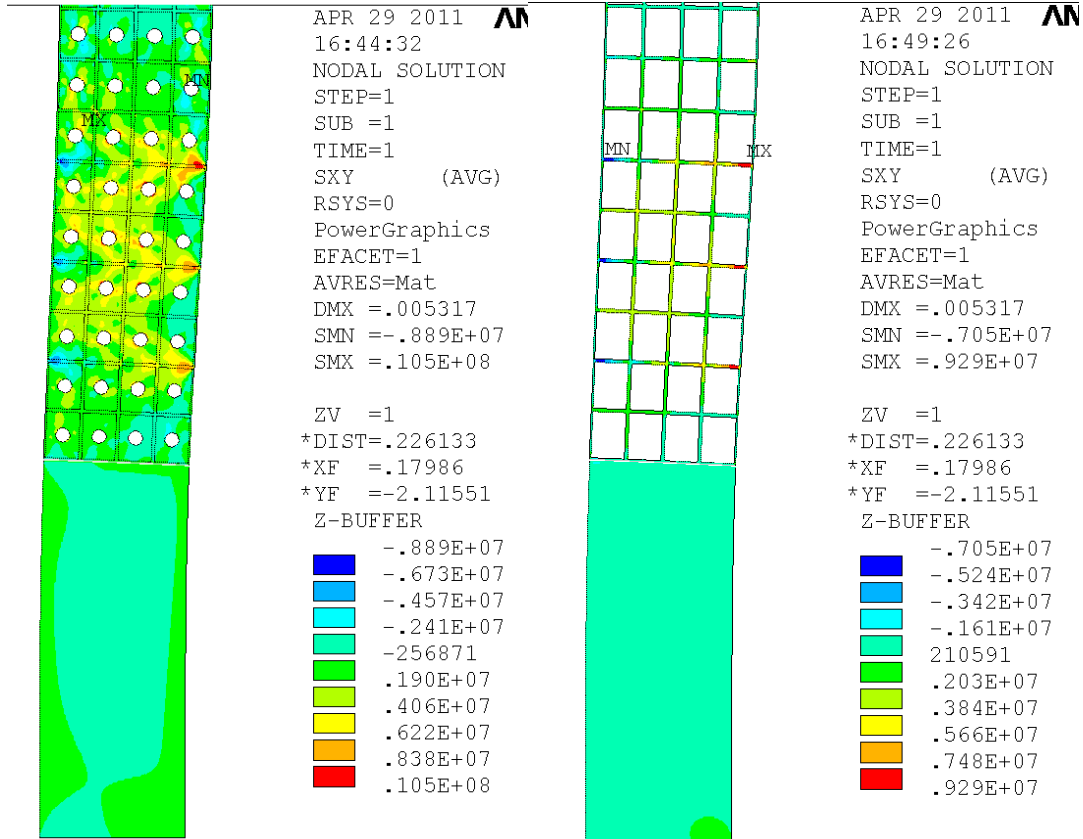
Fig. 18: Vertical stress in the coil due to cooling wave in the bottom of the OH coil

Fig. 19: Shear stress in the coil due to cooling wave in the bottom of the OH coil

The stress in the epoxy insulation in some small areas higher than the static limit of 10 MPa for CTD-101K and certainly higher than its fatigue limit. If CTD-425 insulation system is used with primer, the shear stresses are below the static and fatigue limits. The vertical tensile stress limit in some areas exceed the 10 MPa allowable in the insulation. We recommend the use of a more gradual cooling scheme whereby the starting temperature of the coolant is higher than 12 C and gradually reduced as time progresses. This would reduce the temperature gradients at the beginning of the cooling process in the bottom of the coil and therefore reduce the stresses.

Another temperature gradient scenario of concern is stress in the interface between the OH coil and the G-10 base after the coil has been heated to near 100 Deg. C during a short time while the base is near room temperature. Figure 20 shows the Coil/Base interface geometry in detail. As the hot OH coil thermally expands outward, it is expected to put stress on the interface between the cool G-10 and the coil. Figure 22 shows the insulation and G-10 areas in the model. Note: we added the 2.7mm epoxy ground insulation wrap to the OH coil and the base.
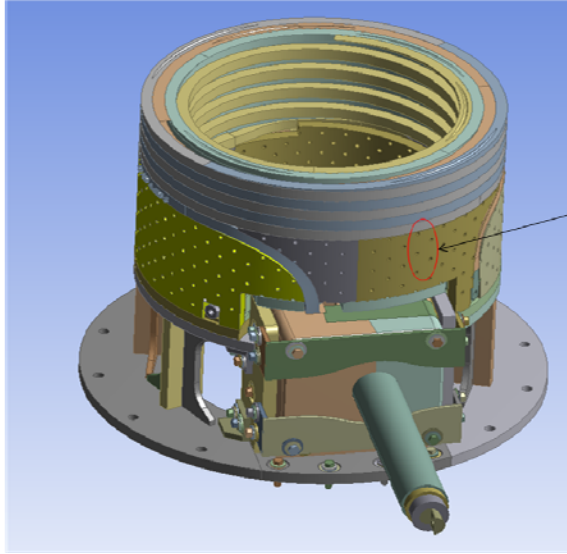
Fig. 20
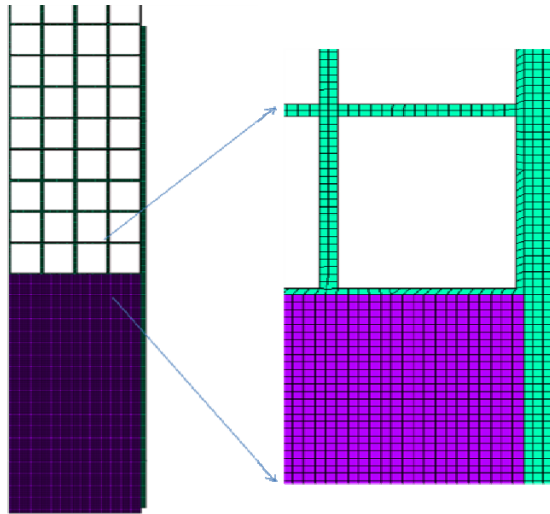
Fig. 22

Figures 23 and 24 show the resulting shear and vertical normal stress contours. It is recommended to put a slip plane at the interface of the base and the outside layer of the coil as pointed out in figure 23.
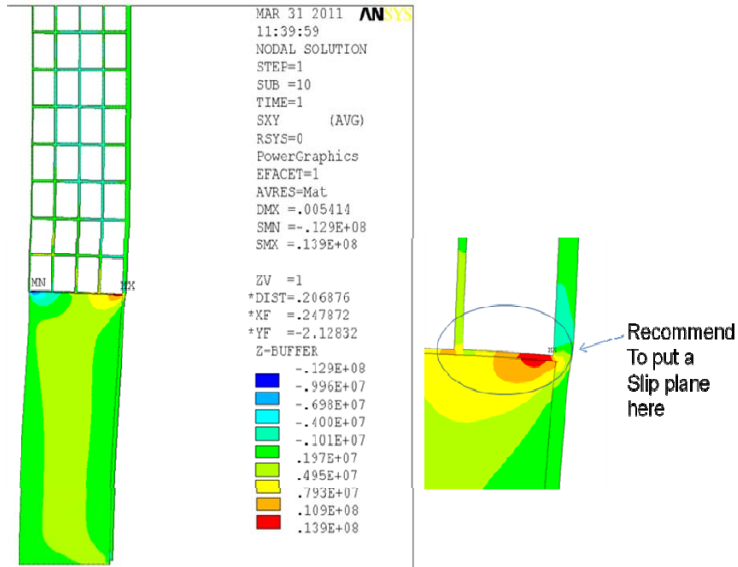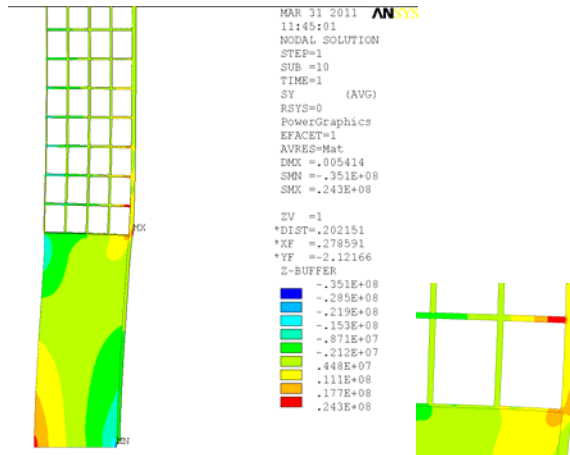
Fig. 23

Fig. 24

Non-Aligned Turns and 3D Effects in OH Coil Interaction with Cold G10 Base:

The top and bottom of the OH coil engages with the G10 not in a linear smooth interface but in a stepped staggered fashion. To model this more accurately in axisymmetry we staggered the turns at the end of the OH by half a turn as shown in Figure 25. The interface between the cold G10 (12 C) and hot coil (91 C) is shown in Figure 25.
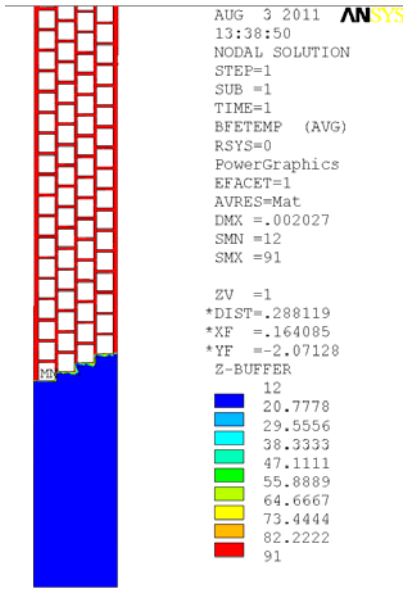
AUG 3 2011 ANSYS
13:38:50
NODAL SOLUTION
STEP=1
SUB =1
TIME=1
BFETEMP (AVG)
RSYS=0
PowerGraphics
EFACET=1
AVRES=Mat
DMX =.002027
SMN =12
SMX =91

ZV =1
*DIST=.288119
*XF =.164085
*YF =-2.07128
Z-BUFFER
        12
        20.7778
        29.5556
        38.3333
        47.1111
        55.8889
        64.6667
        73.4444
        82.2222
        91

Fig. 25

Figure 26 is a contour plot of the XY shear stress in the coil. The maximum shear stress is about 20 MPa and happens at the corner of the turns where the hot turn is surrounded by cold insulation and G10 on two sides. This is confirmed with similar results from the analysis of the OH lead and G0 base area by M. Mardenfeld (see calculation) shown in Figure 27.

AUG 2 2011 ANSYS
16:04:47
NODAL SOLUTION
STEP=1
SUB =1
TIME=1
SXY   (AVG)
RSYS=0
PowerGraphics
EFACET=1
AVRES=Mat
DMX =.00462
SMN =-.205E+08
SMX =.197E+08

ZV =1
*DIST=.250657
*XF =.253007
*YF =-2.11845
Z-BUFFER
        -.205E+08
        -.161E+08
        -.116E+08
        -.711E+07
        -.264E+07
        .184E+07
        .631E+07
        .108E+08
        .153E+08
        .197E+08
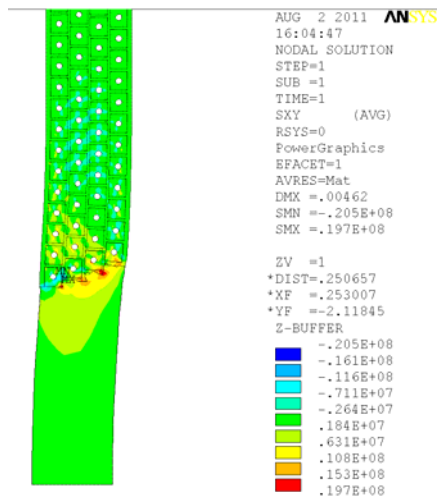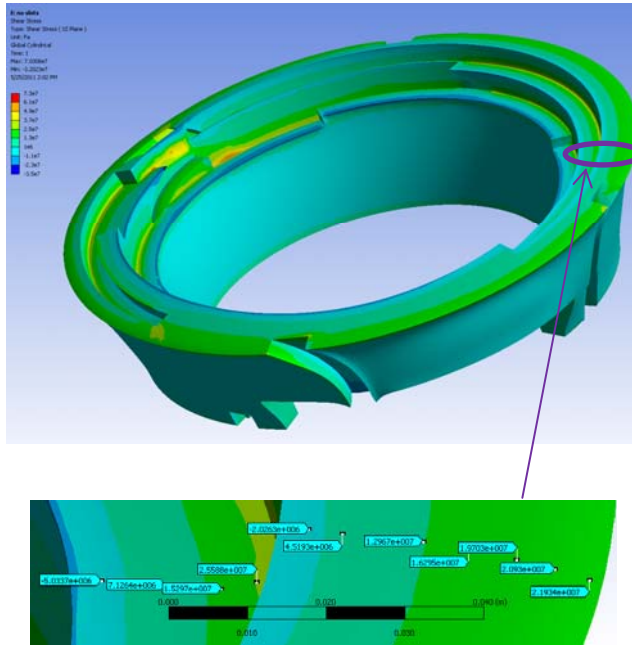
Figure 26

XZ Shear (Pa)

Figure 27

Another area of concern with regard to temperature induced stress at the OH Coil-Base interface is the area of turn to turn brazing of the OH turns at the bottom and top of the coil. The actual geometry of this area is shown in Figure 28. When the OH coil is energized the area of the braze (about 4 inches), where the current carrying conductor is double in area, the heat generation is lower leading to cooler braze area and a resulting temperature gradient in the conductor and the surrounding insulation and G10. To model this effect we built a simplified 3D model of the coil end shown in Figure 29. The two turns in the center of the pack are connected by a 4-in copper braze shown in bright green in Figure 30. Current is input on the turn on the bottom of the brazed area and output from the turn on the top. A multiphysics simulation is run where the heat generation due to electric conduction is fed into a transient thermal simulation (11890 Amps for 6 seconds, equivalent to 24000 Amps for Tesw=1.473 s). Figure 31 is the schematic of the coupled simulation. The temperature results of the thermal simulation is transferred to a static structural Simulation. Figure 32 is a plot of the Joule heating in the pack due to current. Note that the turns on the left and the very top turn in the center have been turned into G10. Figure 33 is a contour plot of temperature in the conductor turns (insulation is turned off in the in the plots). The temperature gradients in the brazed turns are clearly visible. Fig. 34 is a plot of the temperature in the insulation in the middle (along its length) of the coil pack where the colder insulation around the brazed conductors can be seen. Figure 35 is a plot of the shear stress in the insulation. Once again we see large shear stress up to 25MPa at where the hot coil turn is adjacent to a cold insulation and a separation may occur. An investigation (i.e. post mortem analysis) of the existing OH coil would help to shed more light on this king of temperature gradient induced stresses in the insulation.
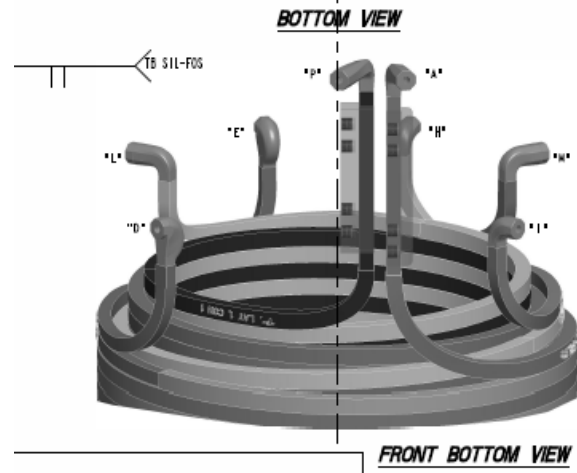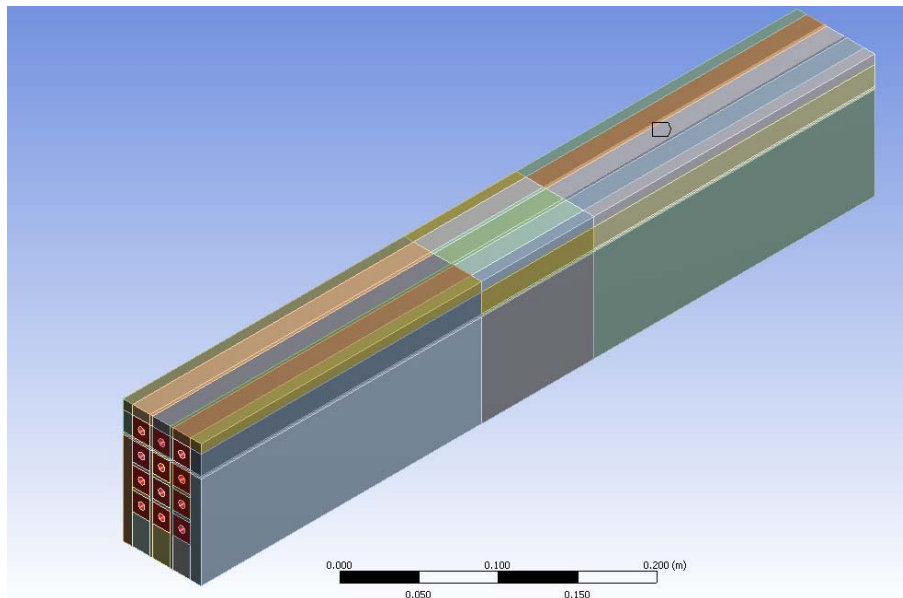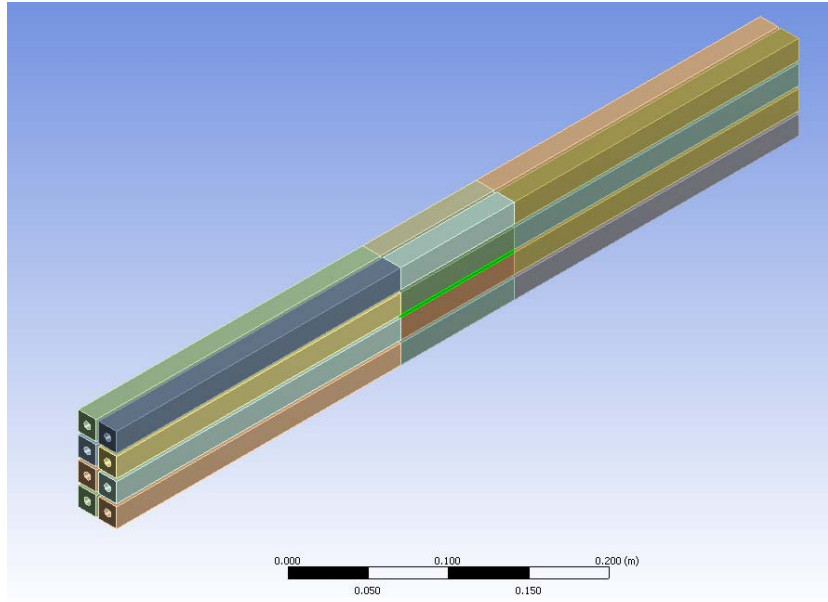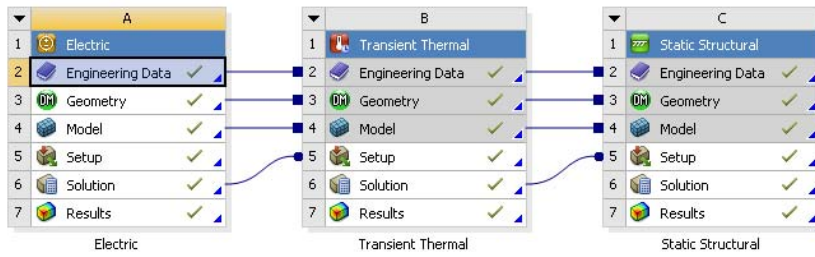
Fig. 28

Fig. 29

Fig. 30

Fig. 31

Fig. 32

Fig. 33

Fig. 34

Fig. 35